Atmospheric and Oceanic Science Letters

ISSN: 1674-2834 (Print) 2376-6123 (Online) Journal homepage: https://www.tandfonline.com/loi/taos20

Interdecadal change in the lagged relationship between the Victoria mode and ENSO

Wei XIE, Guangzhou FAN, Ruiqiang DING, Jianping LI, Baosheng LI, Jianhuang QIN & Xuejing ZHOU

To cite this article: Wei XIE, Guangzhou FAN, Ruiqiang DING, Jianping LI, Baosheng LI, Jianhuang QIN & Xuejing ZHOU (2019) Interdecadal change in the lagged relationship between the Victoria mode and ENSO, Atmospheric and Oceanic Science Letters, 12:4, 294-301, DOI: 10.1080/16742834.2019.1620081

To link to this article: https://doi.org/10.1080/16742834.2019.1620081

© 2019 The Author(s). Published by Informa UK Limited, trading as Taylor & Francis Group.

Published online: 24 May 2019.

Submit your article to this journal

Article views: 567

View related articles

View Crossmark data

Full Terms & Conditions of access and use can be found at
https://www.tandfonline.com/action/journalInformation?journalCode=taos20

ATMOSPHERIC AND OCEANIC SCIENCE LETTERS
2019, VOL. 12, NO. 4, 294–301
https://doi.org/10.1080/16742834.2019.1620081

Taylor & Francis
Taylor & Francis Group

ARTICLE

OPEN ACCESS Check for updates

Interdecadal change in the lagged relationship between the Victoria mode and ENSO

XIE Wei[a,b], FAN Guangzhou[a], DING Ruiqiang[b], LI Jianping[c], LI Baosheng[d], QIN Jianhuang[d] and ZHOU Xuejing[a]

[a]School of Atmospheric Sciences/Plateau Atmosphere and Environment Key Laboratory of Sichuan Province, Chengdu University of Information Technology, Chengdu, China; [b]State Key Laboratory of Numerical Modeling for Atmospheric Sciences and Geophysical Fluid Dynamics, Institute of Atmospheric Physics, Chinese Academy of Sciences, Beijing, China; [c]College of Global Change and Earth System Sciences, Beijing Normal University, Beijing, China; [d]Institute of Oceanography, Shanghai Jiao Tong University, Shanghai, China

ABSTRACT

This paper investigates the interdecadal variability in the lagged relationship between the spring Victoria mode (VM) and the following-winter El Niño–Southern Oscillation (ENSO). It is found that the relationship is strong during high correlation (HC) periods, e.g. 1957–1964 and 1981–2004, but weak during low correlation (LC) periods, e.g. 1907–1924, 1926–1956, 1965–1980, and 2005–2008. The surface air–sea coupling and the evolution of subsurface ocean temperature anomaliesh along the equatorial Pacific associated with the VM are found to be strong during HC periods and weak during LC periods, which results in a stronger impact of the VM on the following-winter ENSO during HC periods. The interdecadal change in the relationship between the VM and ENSO is mainly due to the interdecadal change in the intensity of the VM, which is found to be influenced by the North Pacific Oscillation. Our findings may improve the prediction skill for the onset of ENSO events.

摘要

本文利用1900–2016年的逐月资料，通过相关分析、合成分析等气象统计方法，探讨了VM与ENSO关系的年代际变化。结果表明两者存在显著的年代际变化。在高相关时期，与VM相关的表面海气耦合和沿赤道的次表面海温演变过程均强于低相关时期，导致在高相关时期VM对ENSO的影响更强。此外，进一步分析表明VM-ENSO关系的年代际变化的原因主要是由于VM强度的年代际变化引起的，而VM强度的变化受到北太平洋涛动（NPO）的影响。本文的研究有助于提高ENSO的预报技巧，对于完善ENSO预报的理论框架有进一步的帮助。

ARTICLE HISTORY
Received 20 January 2019
Revised 10 February 2019
Accepted 20 February 2019

KEYWORDS
Victoria mode; ENSO; interdecadal change; North Pacific Oscillation

关键词
维多利亚模态(VM); ENSO; 年代际; 北太平洋涛动(NPO)

1. Introduction

The El Niño–Southern Oscillation (ENSO) is the strongest signal at interannual time scales in Earth's climate system (Philander, Yamagata, and Pacanouski, 1984; Zebiak and Cane 1987). The occurrence and development of ENSO is not only affected by zonal air–sea processes in the western tropical Pacific (e.g. McPhaden and Picaut 1990; McPhaden, Zebiak, and Glantz 2006; Jin 1997a, 1997b; Wyrtki 1975), but also by meridional air–sea processes in the extratropical Pacific (e.g. Ding et al. 2015a; Qin et al. 2017; Wang, Wang, and Zhou 2009). Previous studies have indicated that the North Pacific Oscillation (NPO), as the second leading mode of wintertime atmospheric variability in the North Pacific, is important for interannual ENSO variability as an extratropical forcing source (Rogers 1981; Vimont, Wallace, and Battisti 2003a; Vimont, Battisti, and Hirst 2003b), and that the wintertime NPO can induce an SST footprint onto the ocean, which can persist into late spring and summer, and subsequently forces abnormal westerlies over the equatorial western Pacific, which is conducive to the occurrence of an ENSO event (Vimont, Wallace, and Battisti 2003a; Vimont, Battisti, and Hirst 2003b). Furthermore, some recent studies have indicated that the NPO is closely associated the central Pacific–type El Niño, especially after 1990 (Wang et al. 2018a).

The Victoria mode (VM), as a part of the SST footprint forced by the NPO, is defined as the second empirical orthogonal function mode (EOF2) of monthly sea surface temperature anomalies (SSTAs) in the North Pacific poleward of 20°N (Bond et al. 2003; Ding et al. 2015b). Previous studies imply that the VM in spring, as a response to the forcing of the preceding winter NPO, has an important effect on the following-summer ITCZ (Ding et al. 2015a) precipitation and following-winter ENSO (Ding et al. 2015b). Ding et al. (2015b) further suggested that, rather than being stable, the relationship between the VM and ENSO exhibits significant interdecadal change. Thus, in this work, we investigate the interdecadal variation of the VM–ENSO relationship, and explore the possible causes of the change. The results of the present study

CONTACT Ruiqiang DING drq@mail.iap.ac.cn

© 2019 The Author(s). Published by Informa UK Limited, trading as Taylor & Francis Group.
This is an Open Access article distributed under the terms of the Creative Commons Attribution License (http://creativecommons.org/licenses/by/4.0/), which permits unrestricted use, distribution, and reproduction in any medium, provided the original work is properly cited.

may help understand the effects of extratropical forcing on ENSO.

The remainder of this paper is arranged as follows: Section 2 describes the data and indices. Section 3 demonstrates the interdecadal change in the VM–ENSO relationship and compares atmospheric and oceanic variabilities. Finally, a discussion and summary are provided in Section 4.

2. Data and indices

2.1 Data

We use monthly mean SST data from the HadISST dataset, which is gridded at a horizontal resolution of 1° × 1° (Rayner et al. 2006). The monthly subsurface ocean temperature data are from the SODA reanalysis, version 2.2.4, with a 0.5° × 0.5° horizontal grid resolution and 40 levels in the vertical direction (Giese and Ray 2011). The monthly mean atmospheric dataset is from NOAA's 20th Century Reanalysis, version 2, with a 2° × 2° horizontal grid resolution (Compo et al. 2011).

2.2 ENSO index

The ENSO index (Niño3.4) is defined as the SSTAs averaged over the region (5°S–5°N, 170°–120°W), which has been widely used in recent studies to interpret the change in ENSO intensity. Additionally, in this work, an 11-year high-pass filter is applied to all the data and indices, to remove the interdecadal variability and focus on interannual time scales.

2.3 VM index

Previous studies have implied that the VM peaks in February–April (FMA; Ding et al. 2015b). Therefore, an EOF analysis of the FMA-averaged SSTA field over the North Pacific during 1900–2016 is performed (Figure 1). The spatial pattern of the first mode (EOF1) is closely similar to the Pacific Decadal Oscillation pattern (Zhang, Wallace, and Battisti 1997; Figure 1(a)). The second mode (EOF2), which is the VM, exhibits a distinct dipole structure, with a band of positive SSTAs extending from the west coast of North America to the western Bering Sea, and a band of negative SSTAs over the western-central North Pacific (Figure 1(b); Bond et al. 2003; Ding et al. 2015b). Therefore, we define the normalized time series of EOF2 (Figure 1(b)) as the VM index (VMI).

3. Results

Figure 1(c) shows the interannual anomalies of the FMA (0) VMI (red line) and the following-winter (December–February, DJF) [DJF(+1)] Niño3.4 index (blue line) for 1900–2016. Here, year 0 refers to the year that the VM peaks in FMA and year +1 refers to the following year. We find that the relationship between the FMA(0) VM and the DJF(+1) ENSO is not stationary. These two indices undergo same-sign variations during some decades, but opposite-sign variations during some other decades. Figure 1(d) shows the sliding correlation between the FMA(0) VMI and the DJF(+1) Niño3.4 index with a window of 15 years. The VM–ENSO relationship exhibits a distinct interdecadal variation with significant positive correlations mainly during two periods (1957–1964 and 1981–2004), but with weak correlations during four periods (1907–1924, 1926–1956, 1965–1980, and 2005–2008). These results show that the VM had an enhanced relationship with ENSO during the 1990s, consistent with findings from recent studies (Bond et al. 2003; Yu, Kao, and Tong 2010). It implies that the VM–ENSO relationship varies greatly on the interdecadal time scale, and that the impact of the VM on ENSO is not always strong.

But why exactly does the VM show an enhanced relationship with the subsequent ENSO during some periods, but a much weaker relationship during others? To explore possible causes, the whole period is divided into two groups according to the VM–ENSO relationship: high correlation (HC) periods (1957–1964 and 1981–2004) and low correlation (LC) periods (1907–1924, 1926–1956, 1965–1980, and 2005–2008). Figure 2 shows correlations of the FMA(0) VMI with the following three-month averaged SSTAs and 850-hPa wind anomalies during the HC and LC periods, respectively. During the HC periods, a distinct SSTA pattern with a dipole structure occurs in the North Pacific; meanwhile, a positive SSTA band extends from the eastern North Pacific to the western-central tropical Pacific (Figure 2(a)). Note that anomalous westerlies occur in the subtropical Pacific, while southeasterly wind anomalies occur in the tropical eastern Pacific, causing convergence in the central tropical Pacific that favors the development of positive SSTAs there. This is consistent with the findings of Yu Kao, and Tong (2010) and Wang et al. (2018b). Meanwhile, the positive SSTA band over the subtropical/tropical Pacific combines with negative SSTAs in the western Pacific, resulting in an increased zonal SSTA gradient over the western-central tropical Pacific. This reinforces the abnormal westerlies across this region during June–August (JJA(0)) that trigger the Bjerknes positive feedback process (Bjerknes 1969). Subsequently, the air–sea interaction magnifies zonal wind anomalies and SSTAs over the tropical Pacific. Ultimately, the Niño-like SSTA pattern occurs

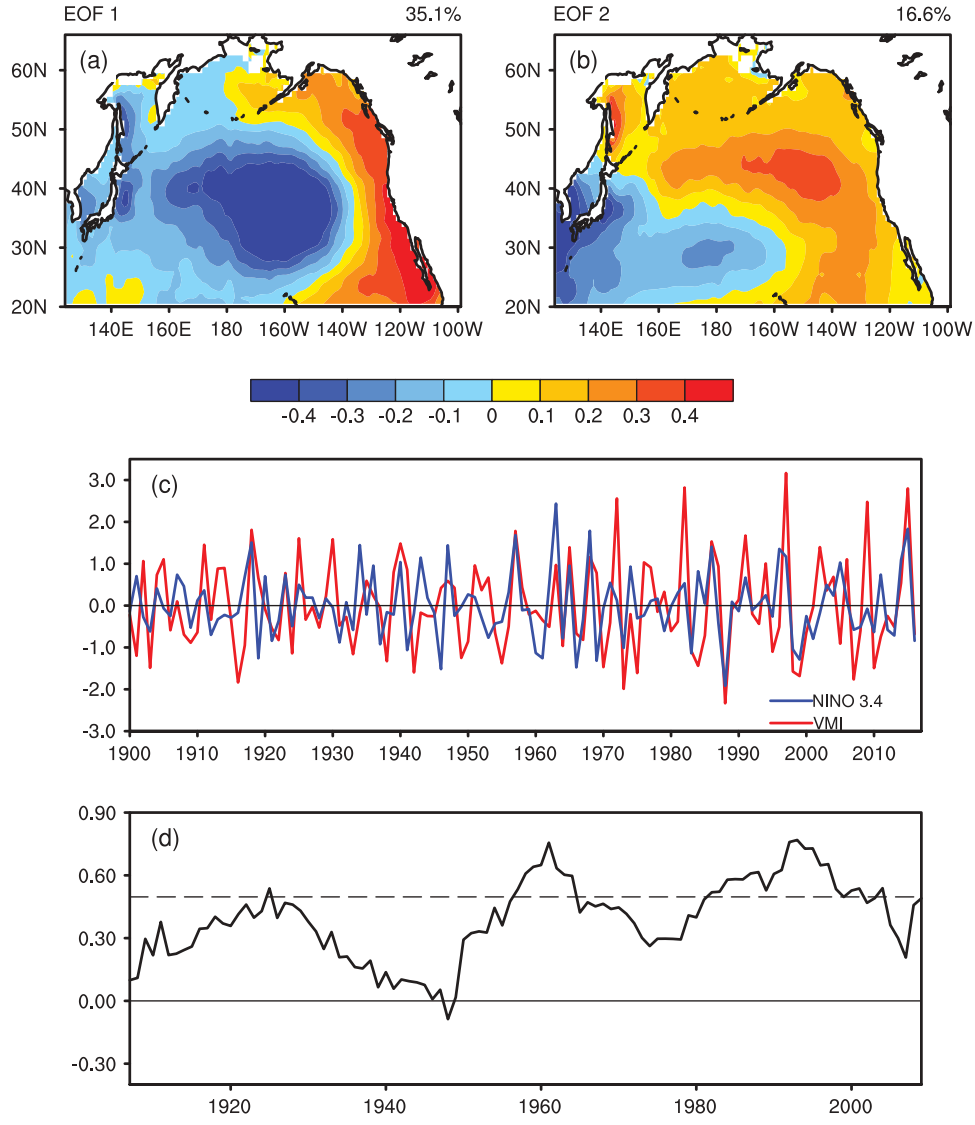

Figure 1. (a) Spatial patterns of the first leading EOF mode of the North Pacific (20.5°–65.5°N, 124.5°E–100.5°W) FMA-averaged SSTA field (after removing the monthly mean global average SSTA). (b) As in (a) but for the second leading EOF mode. (c) Time series of the FMA(0) VMI (red line) and DJF(+1) Niño3.4 index (blue line), after removing the interdecadal variability. (d) The 15-year sliding correlation between the FMA(0) VMI and DJF(+1) Niño3.4 index for the period 1900–2016. The dashed line shows the 95% confidence level.

in the central–eastern equatorial Pacific during DJF (+1), lagging the FMA(0) VMI by 11 months (Figure 2(k)). In contrast, during LC periods, the VM-related SSTAs and wind anomalies are primarily located north of 20°N and do not extend fully to the western-central tropical Pacific. As a result, the abnormal westerly winds in the western-central tropical Pacific do not develop and warming is not established over the central equatorial Pacific, even during August–October (ASO(0); Figure 2(h)).

This result suggests that the VM–ENSO relationship may depend primarily on whether the SSTAs associated with the VM extend fully to the western-central tropical Pacific. If not, it is likely that the VM may exert a relatively weak influence on ENSO.

Figure 3 shows the correlations of the FMA(0) VMI with the following three-month-averaged subsurface ocean temperature anomalies at distinct depths and averaged over the equatorial Pacific (5°S–5°N) for the HC and LC periods. Distinct positive subsurface ocean temperature anomalies occur in the central equatorial Pacific (160°E–160°W) at depths of about 120–300 m when the VM peaks during HC periods (Figure 3(a)). According to the trade wind changing mechanism (Anderson 2004; Anderson, Perez, and Karspeck 2013), these positive subsurface ocean temperature anomalies

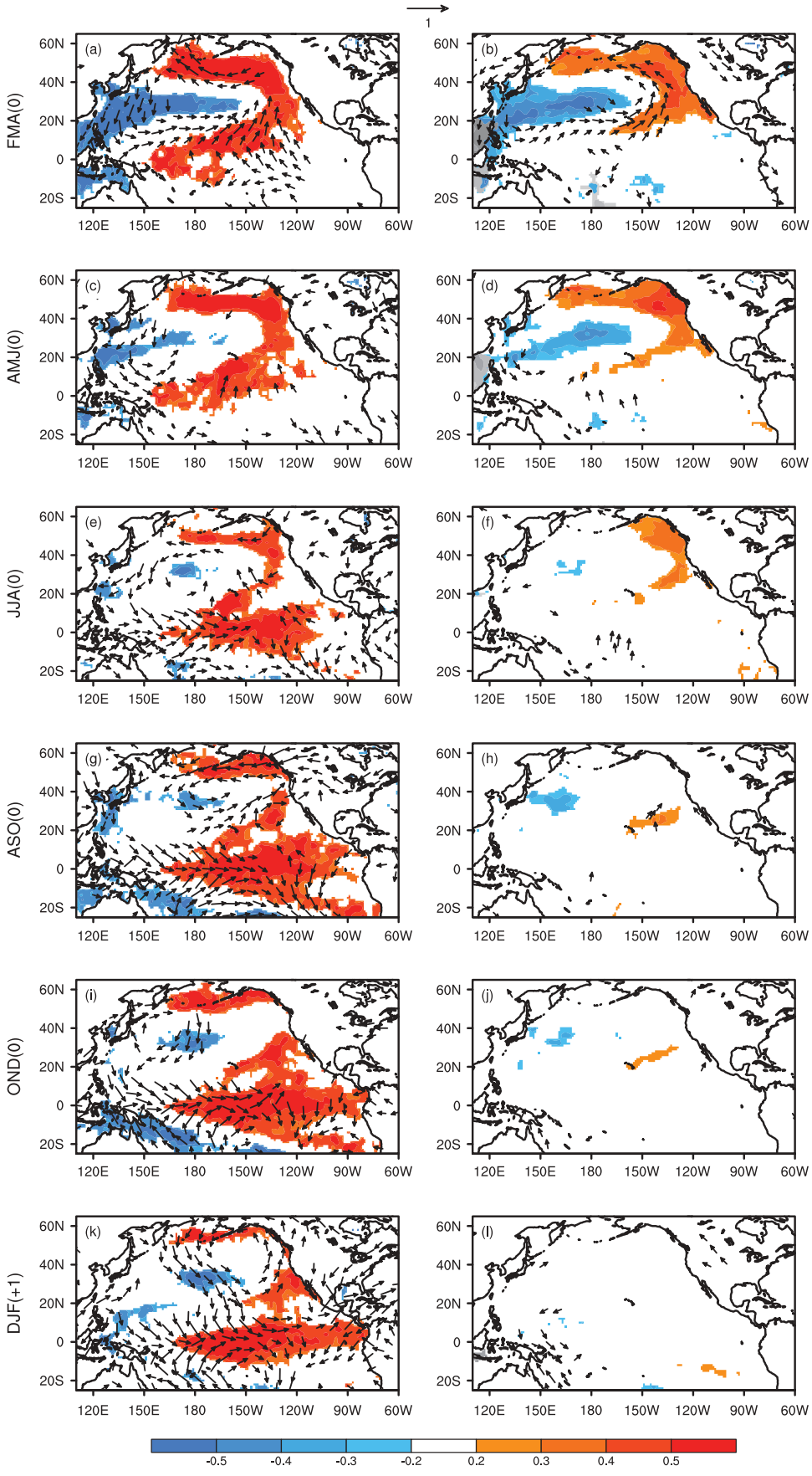

Figure 2. Correlation maps of the three-month averaged SST (shaded) and 850-hPa wind anomalies (vectors) correlated with the FMA(0) VMI for FMA(0), AMJ(0), JJA(0), ASO(0), OND(0), DJF(+1) during the HC (left-hand panels) and LC (right-hand panels) periods. Only SSTAs and 850 hPa wind vectors significant at the 0.05 level are shown.

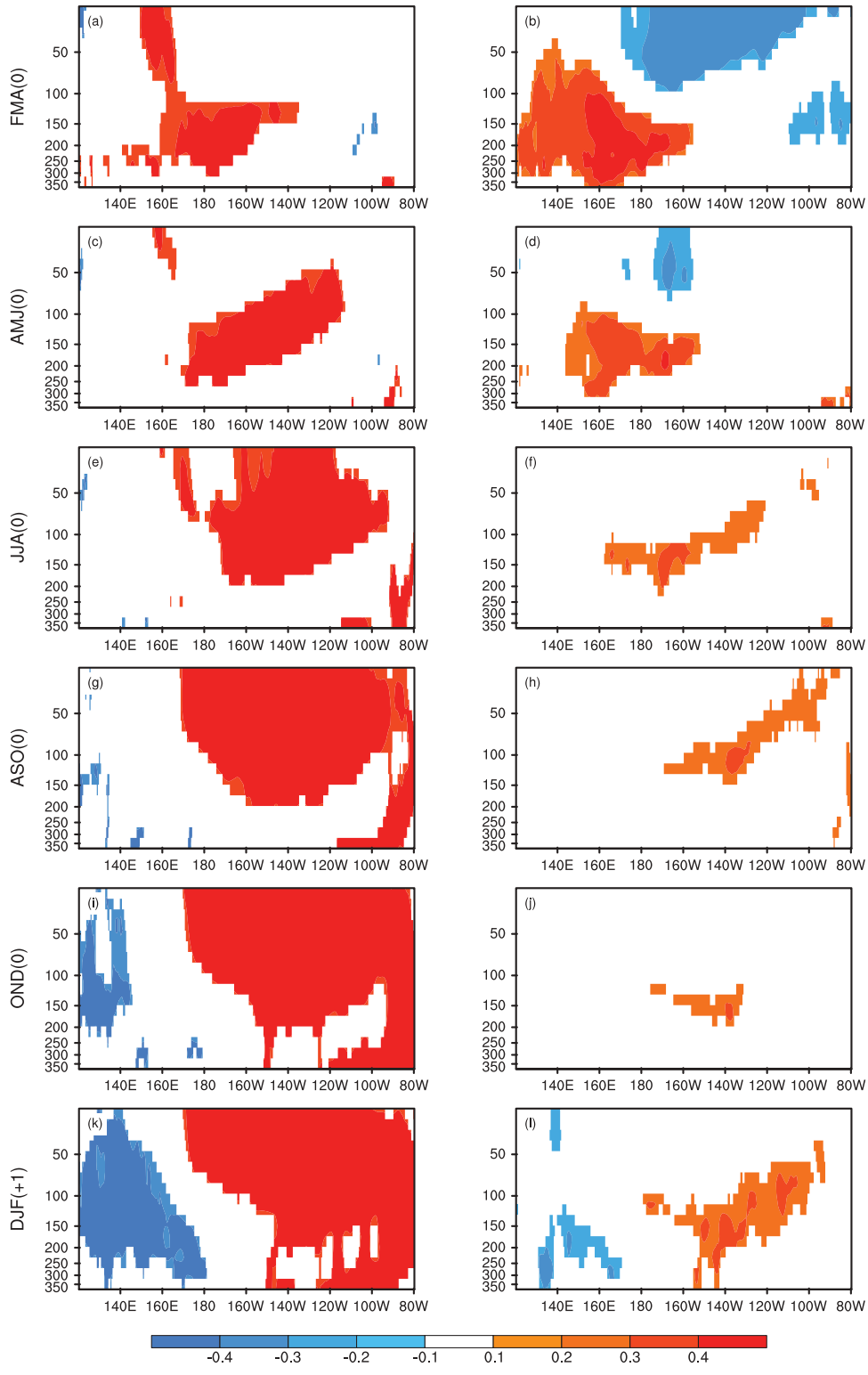

Figure 3. Correlation maps of the FMA(0) VMI with the three-month averaged subsurface ocean temperature anomalies averaged over 5°S–5°N for FMA(0), AMJ(0), JJA(0), ASO(0), OND(0), DJF(+1) during the HC (left-hand panels) and LC (right-hand panels) periods. SSTAs with correlation significant at the 0.05 level are shaded.

are likely aroused by VM-related surface wind anomalies. Subsequently, these subsurface ocean temperature anomalies diffuse upwards and eastwards along the thermocline and subsequently arrive in the eastern equatorial Pacific during AMJ(0) and JJA(0), beginning to warm the surface waters. As a result, the ENSO-like pattern is well established during DJF(+1). In contrast, during LC periods, the propagation of the FMA(0) VM-

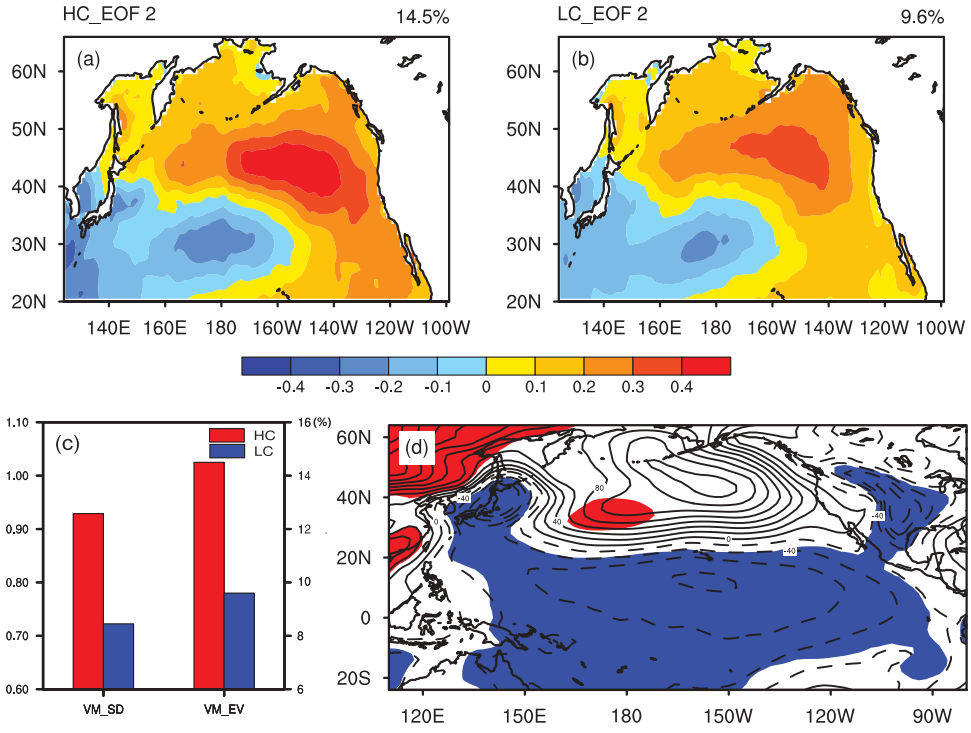

Figure 4. (a) Spatial patterns of the second leading EOF modes of the North Pacific (20.5°–65.5°N, 124.5°E–100.5°W) monthly SSTA field for HC periods (after removing the monthly mean global average SSTA). (b) As (a) but for LC periods. (c) Standard deviation of the FMA(0) VMI and the explained variance of the second leading EOF modes of the North Pacific monthly SSTA field for HC (red bars) and LC periods (blue bars). (d) Composite difference of the December–April-averaged SLP anomaly (contour interval: 0.2 hPa) between the HC and LC periods, with shaded regions significant at the 0.05 level.

related positive subsurface ocean temperature anomalies along the thermocline is weaker, and the relatively weak positive subsurface ocean temperature anomalies cannot reach and therefore warm the surface in the eastern–central Pacific. These conditions may not benefit the formation and maintenance of the ENSO-like SST pattern in the equatorial eastern Pacific.

The results discussed above indicate that there are distinct differences in the intensity of FMA(0) VM-related SSTAs, 850-hPa wind anomalies, and subsurface ocean temperature anomalies between the HC and LC periods. Ding et al. (2015b) reported that the impact of the VM on ENSO may depend on the VM intensity itself. Thus, it is necessary to probe whether it is a change in the intensity of the VM itself that leads to the interdecadal variation in the relationship between the VM and ENSO.

Figure 4(a,b) display the spatial patterns of the EOF2 of the North Pacific monthly SSTA field for the HC and LC periods, respectively. Of note is that the explained variance of the VM pattern is higher for HC periods compared with LC periods (14.5% versus 9.6%). Also, the intensity of the VM during HC periods is stronger than during LC periods (Figure 4(c)). These results imply that the VM is indeed stronger when the lagged VM–ENSO relationship is strengthened.

Since the VM is forced by NPO-like atmospheric forcing, it is of interest to explore whether changes in the intensity of the VM arise from changes in NPO intensity. Because the NPO has a strongest correlation with the VM when the NPO leads the VM for one to two months (Ding et al. 2015b; Alexander et al. 2010), we examine the composite difference of the DJFMA-averaged sea level pressure (SLP) anomalies between the HC and LC periods (Figure 4(d)). The composite SLP pattern resembles the NPO-like pattern, with significant negative anomalies over the North Pacific low latitudes and positive anomalies in the midlatitude North Pacific, suggesting that changes in the NPO intensity may be responsible for the changes in the strength of the VM, which may result in the change of the VM–ENSO relationship.

4. Summary and discussion

Previous studies have indicated that the spring VM exerts a distinct influence on following-winter ENSO events (Ding et al. 2015b). This study suggests that the VM–ENSO relationship exhibits distinct interdecadal variation, with

distinct positive correlations during HC periods (e.g. 1957–1964 and 1981–2004) and weak correlations during LC periods (e.g. 1907–1924, 1926–1956, 1965–1980 and 2005–2008). To explore possible drivers of this interdecadal variation in the VM–ENSO relationship, we compare surface air–sea coupling and subsurface ocean temperature evolutions associated with the VM during HC and LC periods, respectively. During HC periods, distinct positive SSTAs associated with the VM can extend fully into the western–central tropical Pacific, resulting in abnormal westerlies there and subsequent warming of the central–eastern equatorial Pacific during the following winter. In addition, significant positive subsurface ocean temperature anomalies associated with the VM propagate eastwards and upwards, reaching the eastern–central equatorial Pacific and warming the surface ocean. Ultimately, these two processes make the central–eastern equatorial Pacific warm enough to facilitate the onset of ENSO events. In contrast, during LC periods, these two processes are rather weak, and the warming does not establish over the central–eastern equatorial Pacific, even during the following summer. This is not conducive to the occurrence of ENSO events, thereby leading to a weakened relationship between the VM and ENSO during LC periods.

We find that the intensity of the VM during HC periods is stronger than that during LC periods, which implies that the stronger (weaker) VM during HC (LC) periods will tend to result in a stronger (weaker) impact of the VM on ENSO. Furthermore, we demonstrate that changes in the intensity of the VM may be adjusted by the intensity of the NPO. However, our work mainly uses observational and reanalysis data, and so we need to further consider results based on a model. Also, the process by which the NPO affects the VM intensity remains to be further studied.

Disclosure statement

No potential conflict of interest was reported by the authors.

Funding

This research was jointly supported by the National Natural Science Foundation of China [grant number 41790474], the National Program on Global Change and Air–Sea Interaction [grant numbers GASI-IPOVAI-06 and GASI-IPOVAI-03], and the National Key Technology Research and Development Program of the Ministry of Science and Technology of China [grant number 2015BAC03B07].

References

Alexander, M. A., D. J. Vimont, P. Chang, and J. D. Scott. 2010. "The Impact of Extratropical Atmospheric Variability on ENSO: Testing the Seasonal Footprinting Mechanism Using Coupled Model Experiments." *Journal of Climate* 23: 2885–2901. doi:10.1175/2010JCLI3205.1.

Anderson, B. T. 2004. "Investigation of a Large-Scale Mode of Ocean Atmosphere Variability and Its Relation to Tropical Pacific Sea Surface Temperature Anomalies." *Journal of Climate* 17: 4089–4098. doi:10.1175/1520-0442(2004)017<4089:IOALMO>2.0.CO;2.

Anderson, B. T., R. C. Perez, and A. Karspeck. 2013. "Triggering of El Niño Onset through Trade Wind–Induced Charging of the Equatorial Pacific." *Geophysical Research Letters* 40: 1212–1216. doi:10.1002/grl.50200.

Bjerknes, J. 1969. "Atmospheric Teleconnections from the Equatorial Pacific." *Monthly Weather Review* 97: 163–172. doi:10.1175/1520-0493(1969)097<0163:ATFTEP>2.3.CO;2.

Bond, N. A., J. E. Overland, M. Spillane, and P. Stabeno. 2003. "Recent Shifts in the State of the North Pacific." *Geophysical Research Letters* 30: 475. doi:10.1029/2003GL018597.

Compo, G. P., J. S. Whitaker, P. D. Sardeshmukh, N. Matsui, R. J. Allan, X. Yin, B. E. Gleason, et al. 2011. "The Twentieth Century Reanalysis Project." *Quarterly Journal of the Royal Meteorological Society* 137: 1–28. doi: 10.1002/qj.776.

Ding, R., J. Li, Y. H. Tseng, C. Sun, and Y. Guo. 2015b. "The Victoria Mode in the North Pacific Linking Extratropical Sea Level Pressure Variations to ENSO." *Journal of Geophysical Research Atmospheres* 120: 27–45. doi:10.1002/2014JD022221.

Ding, R. Q., J. Li, Y. H. Tseng, and C. Q. Ruan. 2015a. "Influence of the North Pacific Victoria Mode on the Pacific ITCZ Summer Precipitation." *Journal of Geophysical Research Atmospheres* 120: 964–979. doi:10.1002/2014JD022364.

Giese, B. S., and S. Ray. 2011. "El Niño Variability in Simple Ocean Data Assimilation (SODA), 1871–2008." *Journal of Geophysical Research Oceans* 116: C02024.

Jin, F. F. 1997a. "An Equatorial Ocean Recharge Paradigm for ENSO. Part I: Conceptual Model." *Journal of the Atmospheric Sciences* 54: 811–829. doi:10.1175/1520-0469(1997)054<0811:AEORPF>2.0.CO;2.

Jin, F. F. 1997b. "An Equatorial Ocean Recharge Paradigm for ENSO. Part II: A Stripped-Down Coupled Model." *Journal of the Atmospheric Sciences* 54: 830–847. doi:10.1175/1520-0469(1997)054<0830:AEORPF>2.0.CO;2.

McPhaden, M. J., and J. Picaut. 1990. "El-Niño-Southern Oscillation Displacements of the Western Equatorial Pacific Warm Pool." *Science* 250: 1385–1388.

McPhaden, M. J., S. E. Zebiak, and M. H. Glantz. 2006. "ENSO as an Integrating Concept in Earth Science." *Science* 314 (5806): 1740–1745. doi:10.1126/science.1132588.

Philander, S. G. H., T. Yamagata, and R. C. Pacanowski. 1984. "Unstable Air–Sea Interactions in the Tropics." *Journal of the Atmospheric Sciences* 41: 604–613. doi:10.1175/1520-0469-(1984)041<0604:UASIIT>2.0.CO;2.

Qin, J. H., R. Q. Ding, Z. W. Wu, J. Li, and S. Zhao. 2017. "Relationships between the Extratropical ENSO Precursor and Leading Modes of Atmospheric Variability in the Southern Hemisphere." *Advances in Atmospheric Sciences* 34: 1–11. doi:10.1007/s00376-016-6016-z.

Rayner, N. A., N. A. Rayner, P. Brohan, D. E. Parker, C. K. Folland, J. J. Kennedy, M. Vanicek, and S. F. B. Tett. 2006. "Improved Analyses of Changes and Uncertainties in Sea Surface Temperature Measured in Situ since the Mid-Nineteenth Century: The HadSST2 Dataset." *Journal of Climate* 19: 446–469. doi:10.1175/JCLI3637.1.

Rogers, J. C. 1981. "The North Pacific Oscillation." *International Journal of Climatology* 1: 39–57. doi:10.1002/(ISSN)1097-0088a.

Vimont, D. J., D. S. Battisti, and A. C. Hirst. 2003b. "The Seasonal Footprinting Mechanism in the CSIRO General Circulation Models." *Journal of Climate* 16: 2653–2667. doi:10.1175/1520-0442(2003)016<2653:TSFMIT>2.0.CO;2.

Vimont, D. J., J. M. Wallace, and D. S. Battisti. 2003a. "The Seasonal Footprinting Mechanism in the Pacific: Implications for ENSO." *Journal of Climate* 16: 2668–2675. doi:10.1175/1520-0442(2003)016<2668:TSFMIT>2.0.CO;2.

Wang, X., M. Chen, C. Wang, S. W. Yeh, and W. Tan. 2018a. "Evaluation of Performance of CMIP5 Models in Simulating the North Pacific Oscillation and El Niño Modoki." *Climate Dynamics*. doi:10.1007/s00382-018-4196-1.

Wang, X., C. Y. Guan, R. X. Huang, W. Tan, and L. Wang. 2018b. "The Roles of Tropical and Subtropical Wind Stress Anomalies in the El Niño Modoki Onset." *Climate Dynamics*. doi:10.1007/s00382-018-4534-3.

Wang, X., D. X. Wang, and W. Zhou. 2009. "Decadal Variability of Twentieth Century El Niño and La Niña Occurrence from Observations and IPCC AR4 Coupled Models." *Geophysical Research Letters* 36: L11701. doi:10.1029/2009GL037929.

Wyrtki, K. 1975. "El Niño—The Dynamic Response of the Equatorial Pacific Ocean to Atmospheric Forcing." *Journal of Physical Oceanography* 5: 572–584. doi:10.1175/1520-0485(1975)005<0572:ENTDRO>2.0.CO;2.

Yu, J. Y., H. Y. Kao, and L. Tong. 2010. "Subtropics-Related Interannual Sea Surface Temperature Variability in the Central Equatorial Pacific." *Journal of Climate* 23 (11): 2869–2884. doi:10.1175/2010JCLI3171.1.

Zebiak, S., and M. Cane. 1987. "A Model of El Niño–Southern Oscillation." *Monthly Weather Review* 115 (10): 2262–2278. doi:10.1175/1520-0493(1987)115<2262:AMENO>2.0.CO;2.

Zhang, Y., J. M. Wallace, and D. S. Battisti. 1997. "ENSO-like Interdecadal Variability: 1900–93." *Journal of Climate* 10: 1004–1020. doi:10.1175/1520-0442(1997)010<1004:ELIV>2.0.CO;2.